

# Model Based-Energy Control of a Solar Power Plant With a Supercapacitor for Grid-Independent Applications

Phatiphat Thounthong, *Member, IEEE*

**Abstract**—This paper proposes a design for a renewable-energy hybrid power plant that is fed by a photovoltaic (PV) source with a supercapacitor (SC) storage device and is suitable for distributed generation applications. The PV array is used as the main generator, and the SC functions as an auxiliary source for supplying the (transient and steady-state) power deficiency of the PV array. For high-power applications, four-phase parallel boost converters and four-phase parallel bidirectional converters are implemented as a PV converter and a storage device, respectively. A reduced-order mathematical model of the PV and SC converters is described for the control of the power plant. Using a nonlinear approach based on the flatness property, we propose a simple solution to the dynamic, stabilization, and robustness problems in the hybrid power system. This is the key innovative contribution of this research paper. We analyze a prototype small-scale power plant composed of a 0.8-kW PV array and a 100-F SC module. The experimental results authenticate the excellent control algorithm during load cycles.

**Index Terms**—Converters, flatness, hybrid source, nonlinear control, photovoltaic (PV), supercapacitor (SC).

## I. INTRODUCTION

CURRENTLY, renewable energy is receiving greater attention as a sustainable alternative to more traditional energy sources. One of these environmentally friendly energy sources is solar energy; however, there are still some severe concerns about several sources of renewable energy and their implementation, e.g., 1) capital costs and 2) their intermittent power production, called the “intermittency problem.” The intermittency problem of solar energy is that solar panels cannot produce power steadily because their power production rates change with seasons, months, days, hours, etc. If there is no sunlight, no electricity will be produced from the photovoltaic (PV) cell.

To overcome the intermittency problem, a storage medium or electrical energy carrier [a battery or a supercapacitor (SC)]

is needed. An SC storage device is preferable due to its high power density, fast energy sourcing, and long lifetime [1]. In the near future, the utility power system will be supplied on a large scale by solar energy sources and storage device(s) in a *hybrid energy system* to increase the reliability and effectiveness of the individual components [2].

The dynamics, robustness, and stability of the operation of hybrid power plants are of particular interest. In this work, a hybrid power generation system is proposed and it consists of the following main components: a PV source and an SC as a high-power density device. The most popular way to control power converters in the industry today is with a linear control structure [3], [4]. The design of the linear proportional-integral (PI) controller usually proceeds by incorporating the switching mode controller into the plant (converter). Later averaging and linearization enables the employ of the Laplace transform [5], [6]. The PI controller may then be designed for a certain phase margin, normally around 30–60°. Because the switching model of the hybrid power plant (power electronic converters) is nonlinear, it is natural to apply model-based nonlinear control strategies that directly compensate for system nonlinearity without requiring a linear approximation [7].

Currently, many modeling and linear or nonlinear control aspects, including classical state-space or transfer approaches [8], [9], self-tuning methods or sliding mode control [10], the exact linearization technique [11], adaptive control [12], or fuzzy logic-based control [13], have been extensively studied for nonlinear power electronic applications. Flatness-based control has recently been studied in many applications because it is appropriate for robustness, predictive control, trajectory planning, and constraint handling. Based on the flatness approach, the state feedback can be chosen in such a way that the closed-loop dynamic behavior is linear [14]. Flat systems are linearizable in the quasi-static state feedback. When used for tracking, quasi-static state feedback is very useful.

The flatness theory was introduced by Fliess *et al.* [14] in 1995. Recently, these ideas have been used in a variety of nonlinear systems across the various engineering disciplines, including the following applications: the control of an inverted pendulum and a vertical take-off and landing aircraft [15]; the process of a stirred tank chemical reactor [16]; the control of vehicle steering [17]; the control of a high-speed linear axis driven by pneumatic muscle actuators [18]; the control of cathode pressure and the oxygen excess ratio of a proton exchange membrane (PEM) fuel cell system [19]; the steering control of a two-level quantum system [20]; the reactive power and the

Manuscript received March 24, 2011; revised July 6, 2011; accepted September 6, 2011. Date of publication October 10, 2011; date of current version November 23, 2011. This work was supported in part by the research program in cooperation with the Thai–French Innovation Institute, King Mongkut’s University of Technology North Bangkok with the Institut National Polytechnique de Lorraine, Nancy University, under the “Franco-Thai on Higher Education and Research Joint Project year: 2009–2010,” and in part by the Thailand Research Fund under Grant MRG5380261. Paper no. TEC-00153-2011.

The author is with the Department of Teacher Training in Electrical Engineering (TE), King Mongkut’s University of Technology North Bangkok (KMUTNB), Bangkok 10800, Thailand (e-mail: phatiphat.thounthong@ensem.inpl-nancy.fr).

Color versions of one or more of the figures in this paper are available online at <http://ieeexplore.ieee.org>.

Digital Object Identifier 10.1109/TEC.2011.2168400

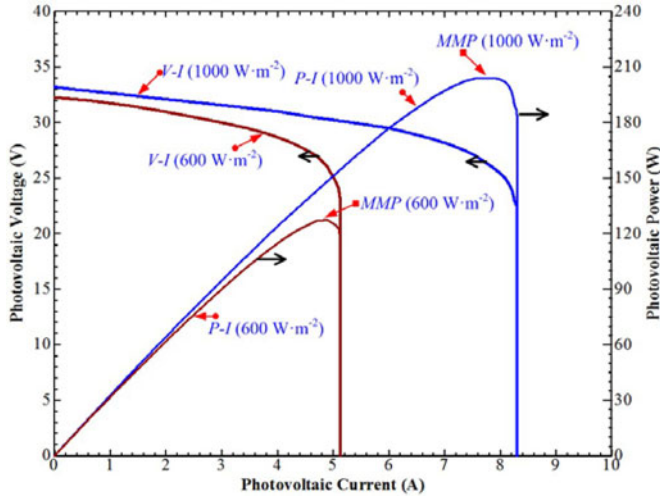


Fig. 1. Power versus current characteristics and voltage versus current characteristics based on a 200-W PV module by the Ekarat Solar at fixed ambient temperature and variable insolation ( $1000$  and  $600 \text{ W}\cdot\text{m}^{-2}$ ).

dc voltage tracking control of a three-phase voltage source converter [21]; the control of open-channel flow in an irrigation canal [22]; and the current control for three-phase three-wire boost converters [23].

We now study an uncomplicated design of a control system of the PV/SC power plant based upon the physical structure of the model. The main contribution of this paper is to present the differential flatness-based control approach of a solar power generation system with an SC storage device. In particular, we do not restrict ourselves to linear control techniques at an equilibrium point. This is the novel work in this domain. The remaining of the paper is structured as follows: the next section describes the hybrid energy system and the power plant model that is studied in this work. In Section III, the proposed energy management algorithm is presented. In Section IV, a proof of the flat system consisting of the solar energy power plant, the control laws, and the system stability is presented. In Section V, the test bench results for the proposed system are presented. Finally, this paper ends with concluding remarks for further study in Section VI.

## II. POWER SOURCE CHARACTERISTICS

### A. Photovoltaic

The PV effect is a basic physical process through which solar energy is converted directly into electrical energy. The physics of a PV cell, or solar cell, is similar to the classical p-n junction diode. The  $V$ - $I$  and  $P$ - $I$  characteristic curves of the PV model used in this study (200-W PV Module by the Ekarat Solar Company) under different irradiances (at  $25^\circ\text{C}$ ) are given in Fig. 1. As shown in Fig. 1, the higher the irradiance, the larger the short-circuit current  $I_{SC}$  and the open-circuit voltage  $V_{OC}$ . As a result, the output PV power will also be larger.

*Remark 1:* PV power systems require some specific estimation algorithms to deliver the maximum power point (MPP) [24], [25]. Because of the typical low-efficiency characteristics of PV panels, it is very important to deliver the maximum instantaneous power from these energy sources to the load with

minimum power conversion for space or terrestrial applications. Temperature also plays an important role in the PV array performance. The lower the temperature, the higher the maximum power and the larger the open-circuit voltage. It is obligatory to use dc/dc or dc/ac converters with effective MPP tracking (MPPT) techniques [26].

### B. Supercapacitor

The SC (or double-layer capacitor or ultracapacitor) is an emerging technology in the field of energy-storage systems. Recent breakthroughs in construction methods aimed at maximizing rated capacitance have provided tremendous increases in the energy-storage capabilities of the double-layer capacitor [27]. With a time constant (the product of equivalent series resistance (ESR) and capacitance) of  $0.001$ – $2$  s for an SC, the stored energy can be extracted at a very high rate because the ESR inside an SC is very small [28]. In contrast, the same-sized battery will not be able to supply the necessary energy in the same time period because of the higher time constant of the battery [27], [29].

The operating voltage of an SC changes linearly with time during constant current operation so that the state-of-charge can be precisely estimated. In addition, the highly reversible electrostatic charge storage mechanism in SCs does not lead to the volume changes observed in batteries with electrochemical transformations of active masses. This volume change usually limits the lifetime cycle of batteries to several hundred cycles, whereas SCs have demonstrated from hundreds of thousands to many millions of full charge/discharge cycles [30], [31].

The SC bank is always connected to the dc bus by means of a two-quadrant dc/dc converter (bidirectional converter). Fig. 2 presents the transient response of an SC converter interfacing between the dc bus and the SC bank (SAFT SC module:  $292 \text{ F}$ ,  $30 \text{ V}$ ) [32]. The initial voltage of the SC bank is  $30 \text{ V}$ . The SC current set-point (reference) is Ch2 and the measured SC current is Ch4. The dynamic response of the SC auxiliary source is very fast and can discharge from  $0$  to  $50 \text{ A}$  in  $0.4 \text{ ms}$ .

*Remark 2:* To operate the SC module, its module voltage is limited to an interval  $[V_{SC\min}, V_{SC\max}]$ . The higher  $V_{SC\max}$  value of this interval corresponds to the rated voltage of the storage device. In general, the lower  $V_{SC\min}$  value is chosen as  $V_{SC\max}/2$ , where the remaining energy in the SC bank is only  $25\%$  and the SC discharge becomes ineffective [32].

## III. SOLAR POWER PLANT

### A. Structure of the Studied Power Converters

Low-voltage, high-current (power) converters are needed because of the electrical characteristics of the PV cell and the SC bank. A classical boost converter is often used as a PV converter [33], and a classical two-quadrant (bidirectional) converter is often used as an SC or battery converter [27]. However, the classical converters will be limited when the power increases or at higher step-up ratios. Therefore, the use of parallel power converters (multiphase converters in parallel) with interleaving may offer better performance in terms of dynamics [34], because

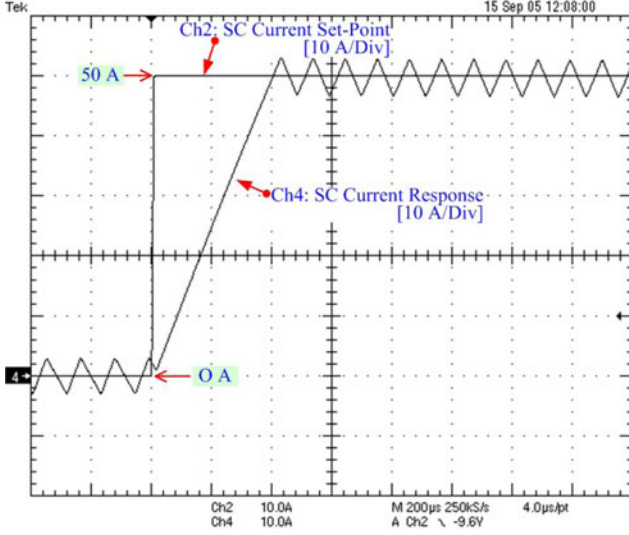


Fig. 2. SC current response to a 0–50 A step (discharging).

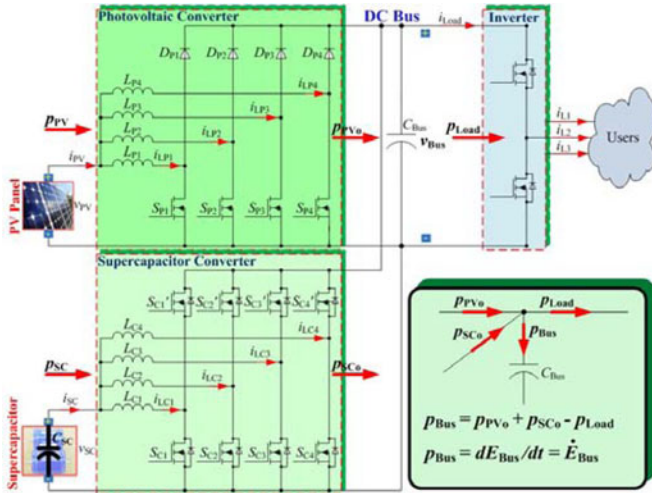


Fig. 3. Proposed circuit diagram of the distributed generation system supplied by a PV and SC, where  $p_{Load} (= v_{Bus} \times i_{Load})$ ,  $v_{Bus}$ , and  $i_{Load}$  are the load power, the dc-bus voltage, and the dc-bus load current, respectively.  $p_{PV} (= v_{PV} \times i_{PV})$ ,  $v_{PV}$ , and  $i_{PV}$  are the PV power, voltage, and current, respectively.  $p_{SC} (= v_{SC} \times i_{SC})$ ,  $v_{SC}$ , and  $i_{SC}$  are the SC power, voltage, and current, respectively.  $p_{PVo}$  and  $p_{SCo}$  are the output powers to the dc link from the converters of the PV array and the SC, respectively.

of smaller inductor and capacitor sizes. Next, Fig. 3 depicts the proposed hybrid source structure. The PV converter combines four-phase parallel boost converters with interleaving, and the SC converter employs four-phase parallel bidirectional converters with interleaving.

### B. Power Regulation Loops of the Proposed Power Plant

For safety and dynamics, the PV and SC converters are primarily controlled by inner current regulation loops (or power regulation loops), as depicted in Figs. 4 and 5 [32]. These power control loops are supplied by two reference signals: the SC power reference  $p_{SCREF}$  and the PV power reference  $p_{PVREF}$ , generated by the control laws presented later.

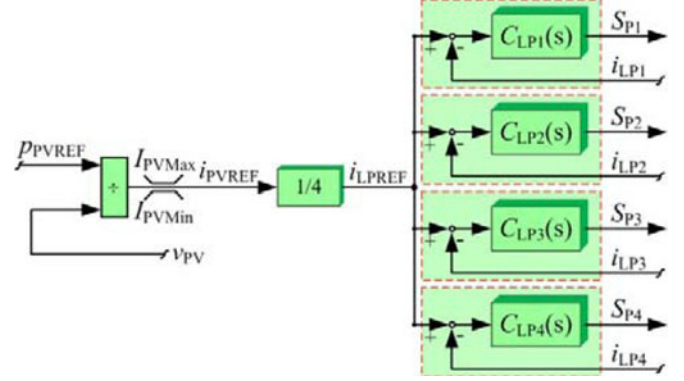


Fig. 4. Photovoltaic power control loop.

For the PV power control, a PV power reference  $p_{PVREF}$  is divided by the measured photovoltaic voltage  $v_{PV}$ , resulting in a PV current reference  $i_{PVREF}$ . For the SC power control loop, an SC power reference  $p_{SCREF}$  is divided by the measured SC voltage  $v_{SC}$  and limited to maintain the SC voltage within an interval  $[V_{SCMin}, V_{SCMax}]$ , according to Remark 2 by the SC current limitation function. This calculation results in an SC current reference  $i_{SCREF}$  [32].

### C. Mathematical Model of the Power Plant

We assume that the PV and SC currents follow their reference values perfectly. Consequently,

$$i_{PV} = i_{PVREF} = \frac{p_{PV}}{v_{PV}} = \frac{p_{PVREF}}{v_{PV}} \quad (1)$$

$$i_{SC} = i_{SCREF} = \frac{p_{SC}}{v_{SC}} = \frac{p_{SCREF}}{v_{SC}} \quad (2)$$

We only consider static losses in these converters, and  $r_{PV}$  and  $r_{SC}$  represent static losses in the PV and SC converters, respectively. Now, the PV array and the SC storage device function as controlled current sources connected with the equivalent series resistance that is called a reduced-order model [35].

The dc-bus capacitive energy  $E_{Bus}$  and the supercapacitive energy  $E_{SC}$  can be written as

$$E_{Bus} = \frac{1}{2} C_{Bus} v_{Bus}^2 \quad (3)$$

$$E_{SC} = \frac{1}{2} C_{SC} v_{SC}^2 \quad (4)$$

The total electrostatic energy  $E_T$  stored in the dc-bus capacitor  $C_{Bus}$  and the SC  $C_{SC}$  can also be written as

$$E_T = \frac{1}{2} C_{Bus} v_{Bus}^2 + \frac{1}{2} C_{SC} v_{SC}^2 \quad (5)$$

Note that the total electrostatic energy  $E_T$  is nearly equal to the energy stored in the SC  $C_{SC}$  because the SC size  $C_{SC}$  is much greater than the dc-bus capacitor size  $C_{Bus}$ .

The derivative of dc-bus capacitive energy  $\dot{E}_{Bus}$  is given versus  $p_{PVo}$ ,  $p_{SCo}$ , and  $p_{Load}$  by the following differential equation:

$$\dot{E}_{Bus} = p_{PVo} + p_{SCo} - p_{Load} \quad (6)$$



where

$$p_{PVo} = p_{PV} - r_{PV} \left( \frac{p_{PV}}{v_{PV}} \right)^2 \quad (7)$$

$$p_{SCo} = p_{SC} - r_{SC} \left( \frac{p_{SC}}{v_{SC}} \right)^2 \quad (8)$$

$$p_{Load} = v_{Bus} \cdot i_{Load}. \quad (9)$$

Note that the derivative of dc-bus capacitive energy  $dE_{bus}/dt$  is the power  $p_{Bus}$  flows into the dc-bus capacitor. It means that  $p_{Bus}$  is equal to  $dE_{bus}/dt$  ( $\dot{E}_{Bus}$ ) (see Fig. 3).

#### IV. CONTROL OF A POWER PLANT

##### A. Energy Balance

In the proposed system depicted in Fig. 3, there are two voltage variables (or two energy variables) to be regulated.

- 1) The dc-bus energy  $E_{Bus}$  is the most important variable.
- 2) The SC storage energy  $E_{SC}$  is the next most important.

Therefore, we propose utilizing SCs, which are the fastest energy source in the proposed system, to supply the energy for the dc bus [32]. In fact, we plan to functionalize the PV array by supplying energy only for charging the SC  $C_{SC}$ . However, during charging, the energy from the PV cell flows through the dc bus to the SC bank. For this reason, the PV array is mathematically operated to supply energy for both the dc-bus capacitor  $C_{Bus}$  and the SC  $C_{SC}$  to keep them charged.

##### B. Differential Flatness Property

Let us first reveal a physical property, used to establish the system flatness [14], [15], [36], that will be the main concept for our reference generations. The flat outputs  $y$ , the control input variables  $u$ , and the state variables  $x$  are defined as

$$\begin{aligned} y &= \begin{bmatrix} y_1 \\ y_2 \end{bmatrix} = \begin{bmatrix} E_{Bus} \\ E_T \end{bmatrix}, \quad u = \begin{bmatrix} u_1 \\ u_2 \end{bmatrix} = \begin{bmatrix} p_{SCREF} \\ p_{PVDEM} \end{bmatrix}, \\ x &= \begin{bmatrix} x_1 \\ x_2 \end{bmatrix} = \begin{bmatrix} v_{Bus} \\ v_{SC} \end{bmatrix} \end{aligned} \quad (10)$$

where  $p_{PVDEM}$  is the PV power demand. It will be generated by the outer controller. This signal will send to an MPPT in order to saturate the PV maximum power. It becomes the PV power reference  $p_{PVREF}$ , presented hereafter.

From (3) and (6), the dc-bus voltage  $v_{Bus}$  (defined as a state variable  $x_1$ ) and the SC power (defined as a control input variable  $u_1$ ) can be expressed as an algebraic function

$$x_1 = \sqrt{\frac{2y_1}{C_{Bus}}} = \varphi_1(y_1) \quad (11)$$

$$\begin{aligned} u_1 &= 2p_{SCLim} \\ &\cdot \left[ 1 - \sqrt{1 - \left( \frac{\dot{y}_1 + i_{Load} \cdot \varphi_1(y_1) - p_{PVo}}{p_{SCLim}} \right)} \right] \\ &= \psi_1(y_1, \dot{y}_1) = p_{SCREF} \end{aligned} \quad (12)$$

$$p_{SCLim} = \frac{v_{SC}^2}{4r_{SC}} \quad (13)$$

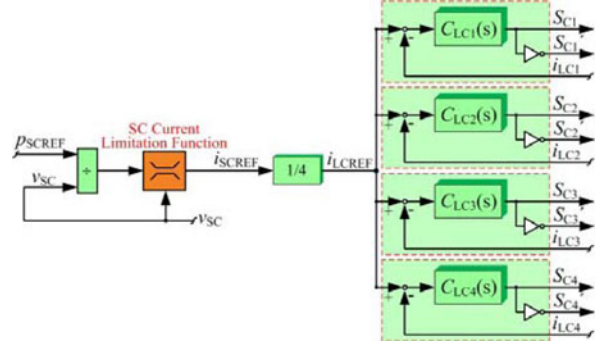


Fig. 5. SC power control loop.

where  $p_{SCLim}$  is the limited maximum power from the SC converter.

From (5) and (6), the SC voltage  $v_{SC}$  (defined as a state variable  $x_2$ ) and the PV power  $p_{PV}$  (defined as a control input variable  $u_2$ ) can be expressed as an algebraic function

$$x_2 = \sqrt{\frac{2(y_2 - y_1)}{C_{SC}}} = \varphi_2(y_1, y_2) \quad (14)$$

$$\begin{aligned} u_2 &= 2p_{PVLim} \cdot \left[ 1 - \sqrt{1 - \left( \frac{\dot{y}_2 + i_{Load} \cdot \varphi_1(y_1)}{p_{PVLim}} \right)} \right] \\ &= \psi_2(y_1, \dot{y}_2) = p_{PVDEM} \end{aligned} \quad (15)$$

$$p_{PVLim} = \frac{v_{PV}^2}{4r_{PV}} \quad (16)$$

where  $p_{PVLim}$  is the limited maximum power from the PV converter.

It is evident that  $x_1 = \varphi_1(y_1)$ ,  $x_2 = \varphi_2(y_1, y_2)$ ,  $u_1 = \psi_1(y_1, \dot{y}_1)$ , and  $u_2 = \psi_2(y_1, \dot{y}_2)$ . Consequently, the PV/SC power plant can be considered a flat system [36].

##### C. Control Law and Stability

Let us now focus our attention on the feedback design to track a dc-bus energy reference trajectory  $y_{1REF}$  and a total energy reference  $y_{2REF}$ . We aim to design a feedback law such that the tracking error  $(y_1 - y_{1REF}, y_2 - y_{2REF})$  asymptotically vanishes. Thus, the relative degree of the first input  $v_1$  and the second input  $v_2$  is 1. The proposed control laws [37] are

$$(\dot{y}_1 - \dot{y}_{1REF}) + K_{11}(y_1 - y_{1REF}) = 0 \quad (17)$$

$$(\dot{y}_2 - \dot{y}_{2REF}) + K_{21}(y_2 - y_{2REF}) = 0. \quad (18)$$

Because the SC can store enormous amount of energy, and the supercapacitive energy is defined as a slower dynamic variable than the dc-bus energy variable, in order to compensate for nonideal effects, an integral term is added to the control law (17). This yields

$$\begin{aligned} v_1 &= \dot{y}_1 = \dot{y}_{1REF} + K_{11}(y_{1REF} - y_1) \\ &+ K_{12} \int_0^t (y_{1REF} - y_1) d\tau \end{aligned} \quad (19)$$

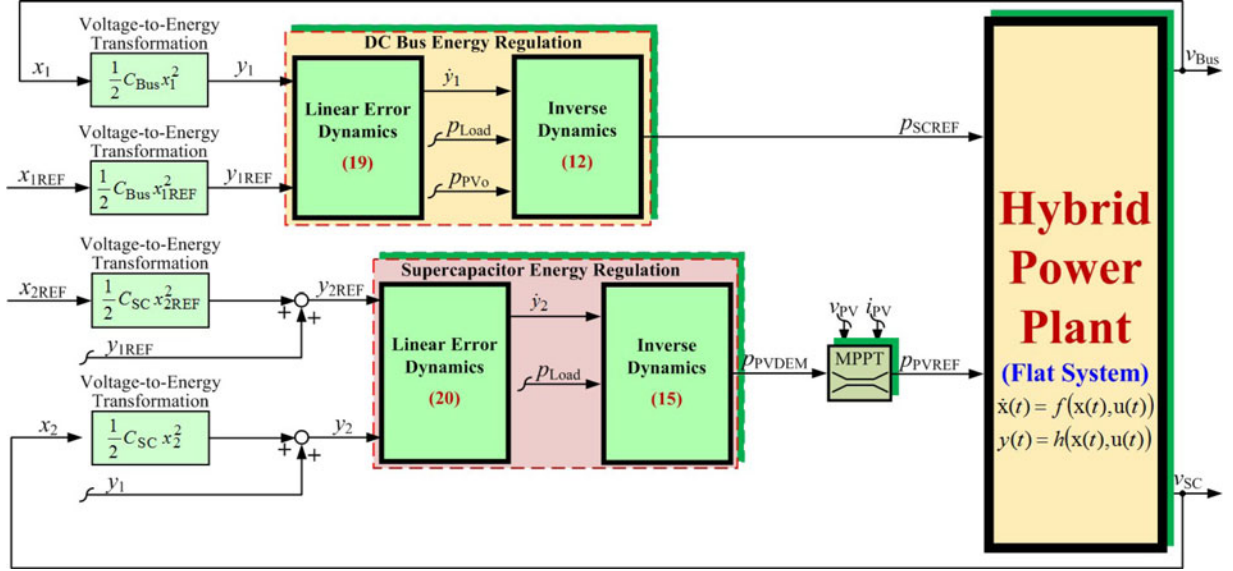


Fig. 6. Multivariable control of a PV/SC hybrid power plant based on a differential flatness approach.

$$v_2 = \dot{y}_2 = \dot{y}_{2REF} + K_{21} (y_{2REF} - y_2). \quad (20)$$

From (19), if we define  $e_1 = y_1 - y_{1REF}$ ,  $K_{11} = 2\zeta\omega_n$ , and  $K_{12} = \omega_n^2$ , we obtain

$$\ddot{e}_1 + 2\zeta\omega_n \cdot \dot{e}_1 + \omega_n^2 \cdot e_1 = 0. \quad (21)$$

Substituting the expression for  $\dot{y}_1$  from (19) into (12) gives the equation for the closed-loop static state feedback SC power.

From (20), if we define  $e_2 = y_2 - y_{2REF}$ ,  $K_{21} = 1/\tau_S$ , we obtain

$$\tau_S \cdot \dot{e}_2 + e_2 = 0. \quad (22)$$

Substituting the expression for  $\dot{y}_2$  from (20) into (15) gives the equation for the closed-loop static state feedback PV power. It is clear that the control system is asymptotically stable for  $K_{11}$ ,  $K_{12} > 0$ , and  $K_{21} > 0$ . However, based on the power electronic constant switching frequency  $\omega_S$  and cascade control structure, the outer control loop (here the dc-bus energy control) must operate at a cutoff frequency  $\omega_E \ll \omega_C \ll \omega_S$ , where  $\omega_C$  is a cutoff frequency of the SC power loop. Once the flat outputs are stabilized, the whole system becomes exponentially stable because all of the variables of the system are expressed in terms of the flat outputs [36].

In Fig. 6, the proposed control algorithm of the renewable energy power plant, as detailed earlier, is depicted. The dc-bus energy control law generates an SC power reference  $p_{SCREF}$  ( $= u_1$ , refer to (12)). The total energy control law (or the SC energy control) generates a PV power demand  $p_{PVDEM}$  ( $= u_2$ , refer to (15)). This signal must be saturated at the maximum power point by MPPT according to *Remark 1*.

It should be concluded here that, in this application, the PV does not always operate at its MPP in a stand-alone (grid-independent) scenario, as depicted in Fig. 6.

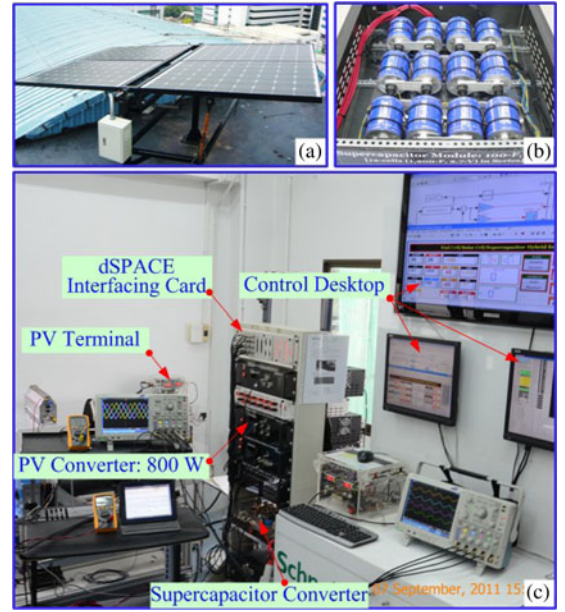


Fig. 7. Photograph of a test bench power plant. (a) solar cell panels, (b) SC bank, and (c) test bench.

## V. PERFORMANCE VALIDATIONS

### A. Power Plant Description for a Test Bench

To validate the performance of the modeling and control system, the small-scale test bench of the hybrid power plant was implemented in our laboratory, as presented in Fig. 7. The prototype 0.8-kW PV converter and the 2-kW SC converter (refer to Fig. 3) were implemented in the laboratory. Specifications of the PV module and storage device are detailed in Table I.

TABLE I  
SPECIFICATIONS OF PHOTOVOLTAIC SOURCE AND STORAGE DEVICE

<b>Photovoltaic Array</b> (by Ekarat Solar Company):			
Number of Panels in Parallel	4		
Panel Open Circuit Voltage	33.5	V	
Panel Rated Voltage	26	V	
Panel Rated Current	7.7	A	
Panel Rated Power	200	W	
Array Rated Power	800	W	
<b>Supercapacitor Bank</b> (by Maxwell Technologies Comp):			
(Cell Model: BCAP1200)			
Number of Cells in Series	12		
Cell Capacity	1,200	F	
Cell Maximum Voltage	2.7	V	
Bank Capacity ( $C_{SC}$ )	100	F	
Bank Maximum Voltage	32	V	

TABLE II  
DC-BUS ENERGY CONTROL LOOP PARAMETERS

$v_{BusREF}$	60	V
$C_{Bus}$	12200	$\mu F$
$K_{11}$	450	$rad \cdot s^{-1}$
$K_{12}$	22,500	$rad^2 \cdot s^{-2}$
$r_{PV}$	0.12	$\Omega$
$r_{SC}$	0.10	$\Omega$
$V_{SCMax}$	32	V
$V_{SCMin}$	15	V
$I_{SCRated}$	150	A

TABLE III  
SUPERCAPACITIVE ENERGY CONTROL LOOP PARAMETERS

$v_{SCREF}$	25	V
$C_{SC}$	100	F
$K_{21}$	0.1	$W \cdot J^{-1}$
$p_{PVMax}$ (Rated)	800	W
$I_{PVMax}$ (Rated)	30.8	A
$I_{PVMin}$	0	A
$\Delta I_{PV}$	0.1	A
$\Delta t$	6	ms

### B. Control Description

The parameters associated with the dc-bus energy regulation loop are summarized in Table II. The parameters associated with the SC energy regulation loop are detailed in Table III. For the low-scale test bench, the dc-bus voltage reference  $v_{BusREF}$  ( $= x_{1REF}$ ) was set to 60 V and the SC voltage reference  $v_{SCREF}$  ( $= x_{2REF}$ ) was set to 25 V (the nominal value of the SC bank).

The constant switching frequency  $\omega_S$  of the PV and SC converters was 25 kHz ( $157\,080 \text{ rad} \cdot s^{-1}$ ). The nonlinear controller gains used were  $K_{11} = 450 \text{ rad} \cdot s^{-1}$  and  $K_{12} = 22\,500 \text{ rad}^2 \cdot s^{-2}$  so that the system damping ratio  $\zeta$  was equal to 1.5 and the natural frequency  $\omega_n$  was equal to  $150 \text{ rad} \cdot s^{-1}$ . As a result, the cutoff frequency  $\omega_E$  of the closed-loop dc-bus energy was equal to  $60 \text{ rad} \cdot s^{-1}$ . This value was lower than the cutoff frequency  $\omega_C$  of the SC power loop of  $450 \text{ rad} \cdot s^{-1}$  (equivalent to a first-order delay with a time constant  $T_C$  of 2.2 ms) so that the system was asymptotically stable [36]. The controller gain of the closed-loop supercapacitive energy was  $K_{21} = 0.1 \text{ W} \cdot J^{-1}$  so that the cutoff frequency  $\omega_{SC}$  of the closed-loop supercapacitive

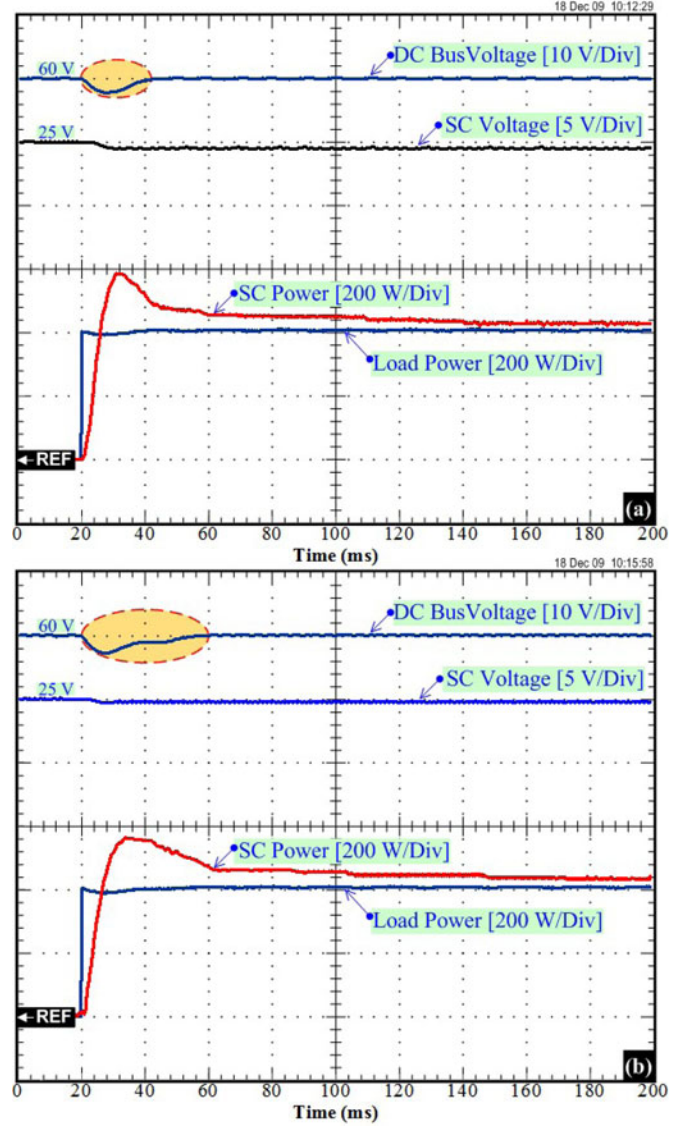


Fig. 8. Comparison of the dc-link stabilization of the power plant during a large load step. (a) Exact model ( $r_{PV} = 0.12 \Omega$ ,  $r_{SC} = 0.10 \Omega$ ). (b) Error model (robustness) ( $r_{PV} = 0.001 \Omega$ ,  $r_{SC} = 0.001 \Omega$ ).

energy was equal to  $0.1 \text{ rad} \cdot s^{-1}$  in which  $\omega_{SC} \ll \omega_E$ , in order to guarantee the asymptotic stability of the whole system.

The PV and SC current regulation loops and the electronic protections were realized by analog circuits. The two energy-control loops, which generate current references  $i_{PVREF}$  and  $i_{SCREF}$ , were implemented in the real-time card dSPACE DS1104 platform (see Fig. 7) using the fourth-order *Runge-Kutta* integration algorithm and a sampling time of  $80 \mu s$  within the mathematical environment of MATLAB-Simulink.

### C. Experimental Results

Because flatness-based control is model based, it may have some sensitivity to error in model parameters. To authenticate its robustness, the flatness-based control was tested with the exact model parameters ( $r_{PV} = 0.12 \Omega$  and  $r_{SC} = 0.10 \Omega$ ) and the erroneous parameters case ( $r_{PV} = 0.001 \Omega$  and  $r_{SC} =$



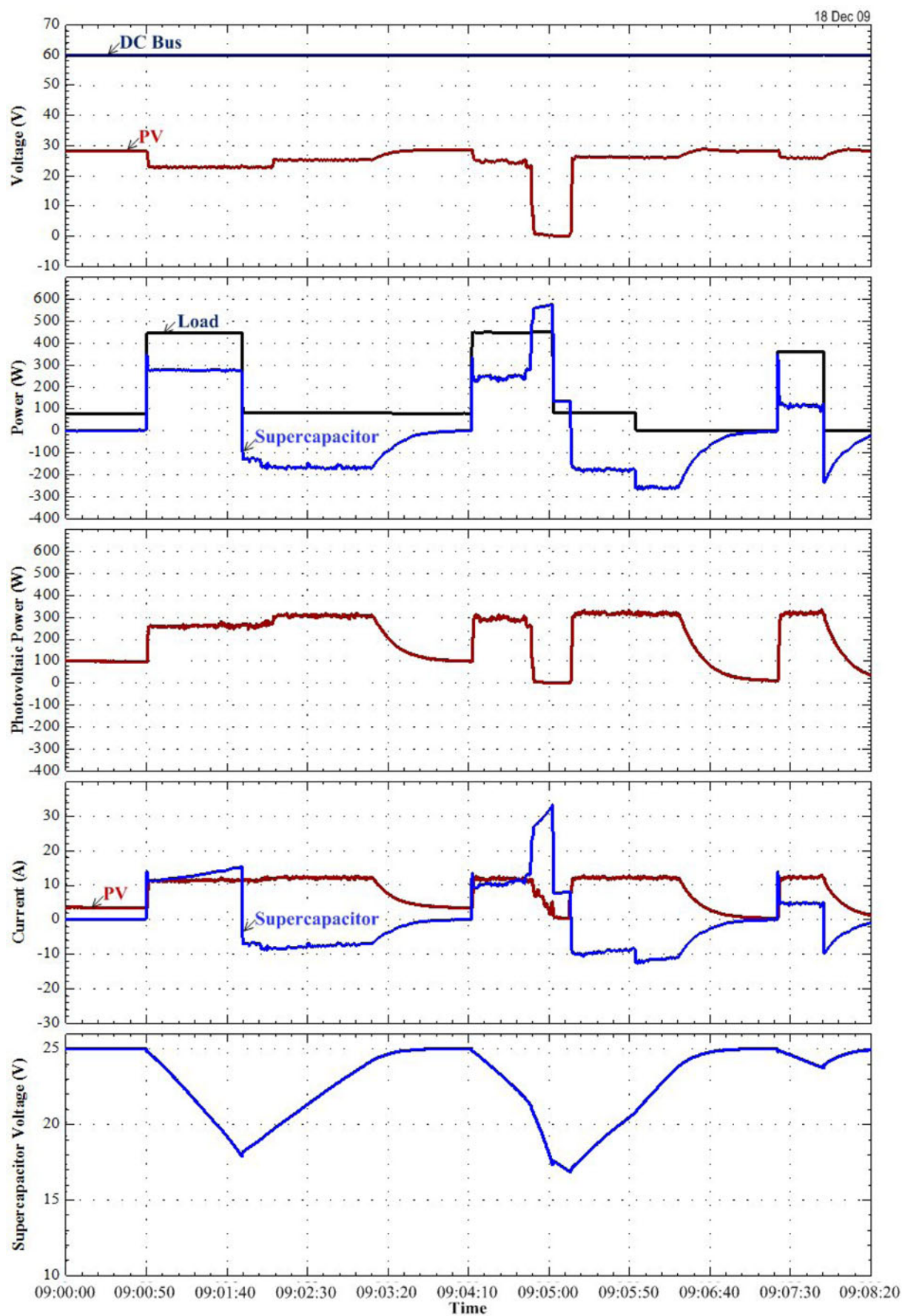


Fig. 9. Experimental results: power plant response during load cycles.

0.001  $\Omega$ ). For the sake of the dc-bus voltage stabilization and robust control system, the oscilloscope waveforms in Fig. 8 show the comparison (robustness) between the accurate parameters and the error parameters. It portrays the dynamic characteristics that are obtained during the large load step. It shows the dc-bus voltage, the load power (disturbance), the SC power, and the SC voltage. The initial state is in no-load power, the SC storage device is full of charge, i.e., the SC voltage = 25 V ( $v_{SCREF} = 25$  V), and the dc-bus voltage is regulated at 60 V ( $v_{BUSREF} = 60$  V); as a result, the PV and SC powers are zero. At  $t = 20$  ms, the large load power steps from 0 W to a constant value of 400 W (positive transition). Because during the transient state the PV power is limited by MPPT estimation, the SC supplies the transient load power demand. One can scrutinize the similar waveforms in Fig. 8(a) and (b). The dc-bus voltage (dc-link stabilization) is minimally influenced by the large load power step. Clearly, the performance of the control system is minimally affected by the model parameter error considered. Experimental testing demonstrates that errors in these parameters had relatively little effect on regulation performance, and we conclude that the nonlinear differential flatness-based approach provides a robust controller in this application.

Finally, for the sake of the dc-bus voltage stabilization and load profile (load cycles), Fig. 9 presents waveforms that are obtained during the load cycles measured on December 18, 2009, at an ambient temperature of around 25 °C. In Fig. 9, the dc-bus voltage, the PV voltage, the load power (disturbance), the SC power, the PV power, the SC current, the PV current, and the SC voltage are shown. In the initial state, the small load power is equal to 100 W, and the storage device is full of charge, i.e.,  $v_{SC} = 25$  V; as a result, the SC power is zero and the PV source supplies 100 W of power for the load. At 09:00:50, the load power steps to the final constant power of around 450 W (positive load power transition). We observe the following phenomena.

- 1) The SC supplies most of the transient power that is required during the step load.
- 2) Simultaneously, the PV power increases to an MPP of around 250 W, which is limited by the MPPT.
- 3) Concurrently, the SC remains in a discharge state after the load step because the steady-state load power (approximately 450 W) is greater than the power supplied by the PV array.

After that phase, one can again observe that the power plant is always energy balanced ( $p_{Load}(t) = p_{PV}(t) + p_{SC}(t)$ ) by the proposed original control algorithm. One can observe that the dc-bus voltage waveform is asymptotically stable during the large load cycles, which is of major importance when employing SC to improve the dynamic performance of the whole system using the proposed control law.

## VI. CONCLUSION AND FURTHER WORKS

The main contribution of this paper is to model and control a PV/SC hybrid power plant. The prototype power plant is composed of a PV array (800 W, Ekarat Solar) and an SC module (100 F, 32 V, Maxwell Technologies). A compact topology,

suitable for high-power applications, is proposed. Its working principle, analysis, and design procedure are presented. The PV array is the main source, and the SC functions as a storage device (or an auxiliary source) to compensate for the uncertainties of the PV source in the steady state and the transient state. An SC can advance the load, following the characteristics of the main sources, by providing a stronger power response to changes in the system load. Adding energy storage to the distributed power systems improves power quality and efficiency.

Using the nonlinear control approach based on the flatness property, we propose a simple solution to the dynamic, stabilization, and robustness problems in the nonlinear power electronic system. And also, there are no operating points comparable with a classical linear control. This is a novel concept for this kind of application. However, the proposed control law needs a load current measurement to estimate the load power. For future work, a load observer will be used to avoid a measurement of a load current, as was explored in [23].

## ACKNOWLEDGMENT

The author would like to thank Dr. P. Sethakul (KMUTNB), Dr. S. Pierfederici, and Dr. B. Davat (Nancy University) for their valuable comments and suggestions about power electronics and control.

## REFERENCES

- [1] Y. Cheng, "Assessments of energy capacity and energy losses of supercapacitors in fast charging–discharging cycles," *IEEE Trans. Energy Convers.*, vol. 25, no. 1, pp. 253–261, Mar. 2010.
- [2] M. Liserre, T. Sauter, and J. Y. Hung, "Future energy systems: Integrating renewable energy sources into the smart power grid through industrial electronics," *IEEE Ind. Electron. Mag.*, vol. 4, no. 1, pp. 18–37, Mar. 2010.
- [3] A. El Aroudi and M. Orabi, "Stabilizing technique for AC–DC boost PFC converter based on time delay feedback," *IEEE Trans. Circuits Syst. II, Exp. Briefs*, vol. 57, no. 1, pp. 56–60, Jan. 2010.
- [4] Suroso and T. Noguchi, "A new three-level current-source PWM inverter and its application for grid connected power conditioner," *Energy Convers. Manage.*, vol. 51, no. 7, pp. 1491–1499, Jul. 2010.
- [5] Y. A. Hajizadeh, M. A. Golkar, and A. Feliachi, "Voltage control and active power management of hybrid fuel-cell/energy-storage power conversion system under unbalanced voltage sag conditions," *IEEE Trans. Energy Convers.*, vol. 25, no. 4, pp. 1195–1208, Dec. 2010.
- [6] L. Ming, C. K. Tse, H. H. C. Iu, M. Xikui, and M. Orabi, "Unified equivalent modeling for stability analysis of parallel-connected DC/DC converters," *IEEE Trans. Circuits Syst. II, Exp. Briefs*, vol. 57, no. 11, pp. 898–902, Nov. 2010.
- [7] P. Thounthong, S. Pierfederici, J.-P. Martin, M. Hinaje, and B. Davat, "Modeling and control of fuel cell/supercapacitor hybrid source based on differential flatness control," *IEEE Trans. Veh. Technol.*, vol. 59, no. 6, pp. 2700–2710, Jul. 2010.
- [8] N. Gyawali and Y. Ohsawa, "Integrating fuel cell/electrolyzer/ultracapacitor system into a stand-alone microhydro plant," *IEEE Trans. Energy Convers.*, vol. 25, no. 4, pp. 1092–1101, Dec. 2010.
- [9] K. Acharya, S. K. Mazumder, and I. Basu, "Reaching criterion of a three-phase voltage-source inverter operating with passive and nonlinear loads and its impact on global stability," *IEEE Trans. Ind. Electron.*, vol. 55, no. 4, pp. 1795–1812, Apr. 2008.
- [10] X. Yu and O. Kaynak, "Sliding-mode control with soft computing: A survey," *IEEE Trans. Ind. Electron.*, vol. 56, no. 9, pp. 3275–3285, Sep. 2009.
- [11] W. K. Na and B. Gou, "Feedback-linearization-based nonlinear control for PEM fuel cells," *IEEE Trans. Energy Convers.*, vol. 23, no. 1, pp. 179–190, Mar. 2008.



- [12] F. Jadot, F. Malrait, J. Moreno-Valenzuela, and R. Sepulchre, "Adaptive regulation of vector-controlled induction motors," *IEEE Trans. Control Syst. Technol.*, vol. 17, no. 3, pp. 646–657, May 2009.
- [13] C.-S. Chiu, "T-S fuzzy maximum power point tracking control of solar power generation systems," *IEEE Trans. Energy Convers.*, vol. 25, no. 4, pp. 1123–1132, Dec. 2010.
- [14] M. Fliess, J. Lévine, Ph. Martin, and P. Rouchon, "Flatness and defect of nonlinear systems: Introductory theory and examples," *Int. J. Contr.*, vol. 61, no. 6, pp. 1327–1361, 1995.
- [15] M. Fliess, J. Lévine, Ph. Martin, and P. Rouchon, "A Lie–Bäcklund approach to equivalence and flatness of nonlinear systems," *IEEE Trans. Automat. Contr.*, vol. 44, no. 5, pp. 922–937, May 1999.
- [16] M. Guay, "On the linearizability of nonisothermal continuous stirred-tank reactors," *Automatica*, vol. 38, no. 2, pp. 269–278, Feb. 2002.
- [17] J. Villagra, B. A. Novel, H. Mounier, and M. Pengov, "Flatness-based vehicle steering control strategy with SDRE feedback gains tuned via a sensitivity approach," *IEEE Trans. Control Syst. Technol.*, vol. 15, no. 3, pp. 554–564, May 2007.
- [18] H. Aschemann and D. Schindele, "Sliding-mode control of a high-speed linear axis driven by pneumatic muscle actuators," *IEEE Trans. Ind. Electron.*, vol. 55, no. 1, pp. 3855–3864, Nov. 2008.
- [19] M. A. Danzer, J. Wilhelm, H. Aschemann, and E. P. Hofer, "Model-based control of cathode pressure and oxygen excess ratio of a PEM fuel cell system," *J. Power Sources*, vol. 176, no. 2, pp. 515–522, Feb. 2008.
- [20] P. S. P. da Silva and P. Rouchon, "Flatness-based control of a single qubit gate," *IEEE Trans. Automat. Contr.*, vol. 53, no. 3, pp. 775–779, Apr. 2008.
- [21] E. Song, A. F. Lynch, and V. Dinavahi, "Experimental validation of nonlinear control for a voltage source converter," *IEEE Trans. Control Syst. Technol.*, vol. 17, no. 5, pp. 1135–1144, Sep. 2009.
- [22] T. Rabbani, S. Munier, D. Dorchies, P. Malaterre, A. Bayen, and X. Litrico, "Flatness-based control of open-channel flow in an irrigation canal using SCADA," *IEEE Control Syst. Mag.*, vol. 29, no. 5, pp. 22–30, Oct. 2009.
- [23] A. Gensior, H. Sira-Ramirez, J. Rudolph, and H. Guldner, "On some nonlinear current controllers for three-phase boost rectifiers," *IEEE Trans. Ind. Electron.*, vol. 56, no. 2, pp. 360–370, Feb. 2009.
- [24] L. R. Chen, C. H. Tsai, Y. L. Lin, and Y. S. Lai, "A biological swarm chasing algorithm for tracking the PV maximum power point," *IEEE Trans. Energy Convers.*, vol. 25, no. 2, pp. 484–493, Jun. 2010.
- [25] T. L. Gibson and N. A. Kelly, "Solar photovoltaic charging of lithium-ion batteries," *J. Power Sources*, vol. 195, no. 12, pp. 3928–3932, Jun. 2010.
- [26] O. Lopez, F. D. Freijedo, A. G. Yepes, P. F. Comesana, J. Malvar, R. Teodorescu, and J. Doval-Gandoy, "Eliminating ground current in a transformerless photovoltaic application," *IEEE Trans. Energy Convers.*, vol. 25, no. 1, pp. 140–147, Mar. 2010.
- [27] A. Khaligh and Z. Li, "Battery, ultracapacitor, fuel cell, and hybrid energy storage systems for electric, hybrid electric, fuel cell, and plug-in hybrid electric vehicles: state of the art," *IEEE Trans. Veh. Technol.*, vol. 59, no. 6, pp. 2806–2814, Jul. 2010.
- [28] J. R. Mille, "Introduction to electrochemical capacitor technology," *IEEE Electr. Insulat. Mag.*, vol. 26, no. 4, pp. 40–47, Jul. 2010.
- [29] V. Agarwal, K. Uthachana, R. A. DeCarlo, and L. H. Tsoukalas, "Development and validation of a battery model useful for discharging and charging power control and lifetime estimation," *IEEE Trans. Energy Convers.*, vol. 25, no. 1, pp. 140–147, Mar. 2010.
- [30] M. Inagaki, H. Konno, and O. Tanaike, "Carbon materials for electrochemical capacitors," *J. Power Sources*, vol. 195, no. 24, pp. 7880–7903, Dec. 2010.
- [31] A. Hammar, P. Venet, R. Lallemand, G. Coquery, and G. Rojat, "Study of accelerated aging of supercapacitors for transport applications," *IEEE Trans. Ind. Electron.*, vol. 57, no. 12, pp. 3972–3979, Dec. 2010.
- [32] P. Thounthong, S. Raël, and B. Davat, "Analysis of supercapacitor as second source based on fuel cell power generation," *IEEE Trans. Energy Convers.*, vol. 24, no. 1, pp. 247–255, Mar. 2009.
- [33] G. Spagnuolo, G. Petrone, S. V. Araujo, C. Cecati, E. Friis-Madsen, E. Gubia, D. Hissel, M. Jasinski, W. Knapp, M. Liserre, P. Rodriguez, R. Teodorescu, and P. Zacharias, "Renewable energy operation and conversion schemes: A summary of discussions during the seminar on renewable energy systems," in *IEEE Ind. Electron. Mag.*, no. 1, vol. 4, Mar. 2010, pp. 38–51.
- [34] P. Thounthong and B. Davat, "Study of a multiphase interleaved step-up converter for fuel cell high power applications," *Energy Convers. Manage.*, vol. 51, no. 4, pp. 826–832, Apr. 2010.
- [35] S. D. Sudhoff, K. A. Corzine, S. F. Glover, H. J. Hegner, and H. N. Robey, Jr., "DC link stabilized field oriented control of electric propulsion systems," *IEEE Trans. Energy Convers.*, vol. 13, no. 1, pp. 27–33, Mar. 1998.
- [36] P. Thounthong, S. Pierfederici, and B. Davat, "Analysis of differential flatness-based control for a fuel cell hybrid power source," *IEEE Trans. Energy Convers.*, vol. 25, no. 3, pp. 909–920, Sep. 2010.
- [37] P. Thounthong and S. Pierfederici, "A new control law based on the differential flatness principle for multiphase interleaved DC–DC converter," *IEEE Trans. Circuits Syst. II, Exp. Briefs*, vol. 57, no. 11, pp. 903–907, Nov. 2010.



**Phatiphat Thounthong** (M'09) received the B.S. and M.E. degrees in electrical engineering from King Mongkut's Institute of Technology North Bangkok (KMUTNB), Bangkok, Thailand, in 1996 and 2001, respectively, and the Ph.D. degree in electrical engineering from the Institut National Polytechnique de Lorraine (INPL)-Nancy University, Nancy-Lorraine, France, in 2005.

He is currently an Associate Professor in the Department of Teacher Training in Electrical Engineering (TE), King Mongkut's University of Technology North Bangkok (KMUTNB). His current research interests include power electronics, electric drives, and electrical devices (fuel cell, solar cell, wind turbine, batteries, and SC).